

[19] *In Vivo* Crosslinking Methods for Analyzing the Assembly and Architecture of Chemoreceptor Arrays

By CLAUDIA A. STUDDERT and JOHN S. PARKINSON

Abstract

The chemoreceptor molecules that mediate chemotactic responses in bacteria and archaea are physically clustered and operate as highly cooperative arrays. Few experimental approaches are able to investigate the structure–function organization of these chemoreceptor networks in living cells. This chapter describes chemical crosslinking methods that can be applied under normal physiological conditions to explore physical interactions between chemoreceptors and their underlying genetic and structural basis. Most of these crosslinking approaches are based on available atomic structures for chemoreceptor homodimers, the fundamental building block for higher-order networks. However, the general logic of our *in vivo* crosslinking approaches is readily applicable to other protein–protein interactions and other organisms, even when high-resolution structural information is not available.

Introduction

Motile bacteria track gradients of attractant and repellent chemicals in the search for optimal living environments. This behavior, known as chemotaxis, involves a signal transduction pathway that has been extensively characterized in *E. coli* [reviewed by (Parkinson *et al.*, 2005; Sourjik, 2004; Szurmant and Ordal, 2004)]. The proteins responsible for sensing chemical gradients are known as methyl-accepting chemotaxis proteins, or MCPs (Zhulin, 2001). These chemoreceptors are homodimeric membrane proteins that typically contain a ligand-specific periplasmic sensing domain, flanked by two trans-membrane regions, and a highly conserved cytoplasmic signaling domain (Fig. 1). MCPs form ternary signaling complexes with CheA, a histidine kinase, and CheW, an adaptor protein that couples CheA to receptor control. Information about receptor ligand occupancy is transmitted across the inner membrane to the cytoplasmic domain, which regulates autophosphorylation of CheA. CheA activity, in turn, regulates the phosphorylation state of the response regulator CheY, which modulates the direction of rotation of the flagellar motors, the final target of the signaling pathway.

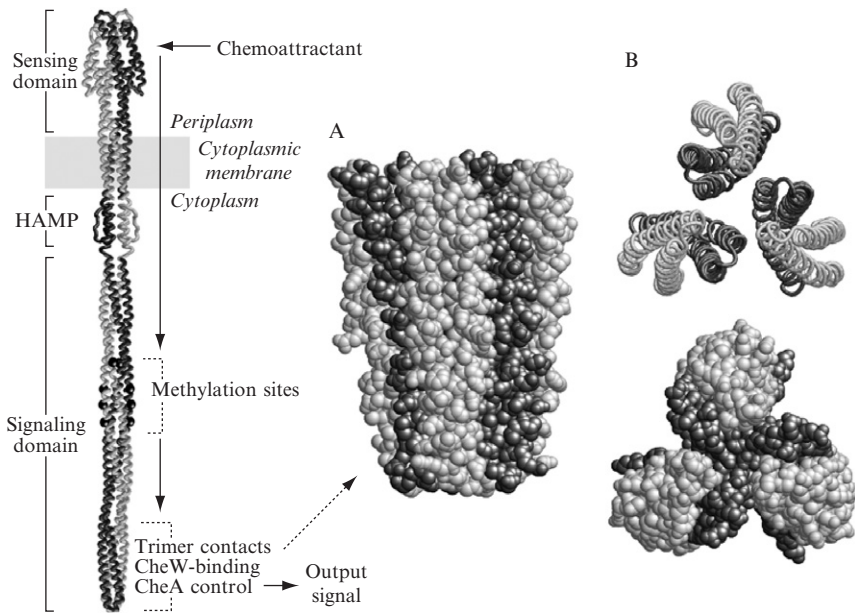


FIG. 1. Functional architecture of MCP-family chemoreceptors. Left: Atomic structure of an MCP homodimer assembled from structures for the Tar ligand-binding domain (Milburn *et al.*, 1991), the Tsr signaling domain (Kim *et al.*, 1999), and the HAMP domain from a non-MCP thermophile protein (Hulko *et al.*, 2006). MCP subunits also carry an unstructured segment at their C-terminus (not shown), whose function is not well understood. High-abundance receptors Tar and Tsr also carry a pentapeptide (not shown) at the end of the C-terminal linker that binds to and modulates the enzymatic activities of CheR and CheB, the MCP modifying enzymes. The backbone traces of the predominantly alpha-helical subunits are shaded differently to show the arrangements and structural interactions within the dimer. Chemoattractants trigger conformational changes in the periplasmic sensing domain that propagate across the cytoplasmic membrane, eventually influencing output signals generated at the cytoplasmic tip of the molecule. The tips of three MCP dimers are thought to associate in a trimer-of-dimers arrangement needed for CheA activation and control. (A) A space-filled side view of the trimer tip. Each dimer has one subunit (dark) that lies at the interdimer interface and contributes nine residues that stabilize the trimer arrangement. The other subunit in each dimer (light) lies mainly on the outside surface of the trimer, but contributes two additional residues to trimer packing interactions. (B) Backbone and space-filled structures of the trimer contact region viewed from the cytoplasmic tip. The shading scheme used in (A) also applies to these images. The structures in (A) and (B) are shown at the same relative scale.

MCPs sense temporal changes in chemoeffector levels by comparing their current occupancy state with that averaged over the past few seconds, recorded in the form of reversible methylation of 4 to 6 glutamic acid residues in the signaling domain. Cells adapt to unchanging chemical

environments by adjusting their MCP methylation levels through the action of a methyltransferase CheR and a methyl-esterase CheB. CheR operates at a substrate-limited rate, whereas CheB is feedback-regulated through phosphorylation signals from the receptor complexes.

E. coli has four MCPs with different detection specificities (Tsr, serine; Tar, aspartate and maltose; Tap, dipeptides; Trg, ribose and galactose) and a fifth MCP-like receptor (Aer) that mediates aerotactic behavior. These chemoreceptors and their associated signaling proteins are localized in clusters, often at the cell poles, in *E. coli* (Maddock and Shapiro, 1993; Sourjik and Berg, 2000) and in a variety of other bacteria (Gestwicki *et al.*, 2000). Clustering may enable receptor molecules to exchange sensory information and thereby act cooperatively to amplify small chemical stimuli into large flagellar-controlling output signals (Bray *et al.*, 1998; Sourjik and Berg, 2002, 2004). Although many genetic and biochemical studies have contributed to an understanding of the general organization of chemoreceptor clusters and their underlying protein–protein interactions, the assembly and architecture of chemoreceptor clusters are not well understood.

An interesting clue to the possible nature of receptor–receptor interactions was provided by the crystal structure of the Tsr signaling domain, which revealed a trimer-of-dimers arrangement (Kim *et al.*, 1999) (Fig. 1B). The eleven residues principally involved in dimer–dimer contacts at the trimer interface are identical in all five *E. coli* MCP-family transducers, suggesting that the trimer arrangement might be a structural and functional component of receptor signaling clusters.

Crosslinking methods can be used to map protein–protein interactions. The availability of a large variety of crosslinkers, together with many analytical tools for characterizing the crosslinking products, makes it a versatile and reliable approach that permits inspection of macromolecular assemblies as they are found *in vivo*. This chapter focuses on the crosslinking methods that we have used to assess whether functional chemoreceptors are organized in trimers of dimers in intact cells, to characterize the interactions between receptors of different specificities, and to study the dynamics of those interactions under different cellular conditions.

Use of a Lysine-Targeted Crosslinker to Probe Receptor–Receptor Interactions in Cells

DSP [di-thiobis(succinimidyl propionate)] is a bifunctional, lysine-reactive reagent with a relatively short spacer arm (11–12 Å). DSP crosslinks are reversible, owing to the presence of a disulfide bridge connecting the two succinimide moieties. DSP crosses biological membranes, so it can potentially trap any two proteins that reside close together in the cell, provided

that they both contain lysine residues at an appropriate distance. Since lysine is a relatively common residue in proteins, DSP is a good candidate to use for a preliminary search of uncharacterized protein interactions. In fact, the first attempt to analyze interactions between chemotaxis proteins in intact cells made use of DSP (Chelsky and Dahlquist, 1980). Several oligomeric forms of different chemotaxis proteins were identified in that pioneering study. Notably, the MCPs Tar and Tsr formed DSP-crosslinked products of up to four subunits (Chelsky and Dahlquist, 1980).

We used DSP to show that Tar and Tsr molecules are physically associated in intact cells (Ames *et al.*, 2002). The experimental steps are depicted in Fig. 2. A Tar receptor carrying a 6× His tag (Tar-6× His) was coexpressed at physiological levels with a nontagged Tsr and cells in the midlog phase of growth were treated with DSP. After the treatment, membrane proteins were solubilized with a detergent, and all His-tagged molecules (together with any covalently attached proteins) were purified on a nickel resin column. His-tagged products were then treated with a reducing agent to break crosslinks and the individual protein components were analyzed by SDS-PAGE and visualized by immunoblotting with a polyclonal antiserum directed against a highly conserved segment of the MCP signaling domain.

To distinguish Tar and Tsr molecules, we used a gel system in which they had different mobilities. To simplify the resulting band patterns, we used a host strain that lacked the MCP-modifying CheR and CheB enzymes so that all receptor molecules were in the unmodified state. Comparing the protein

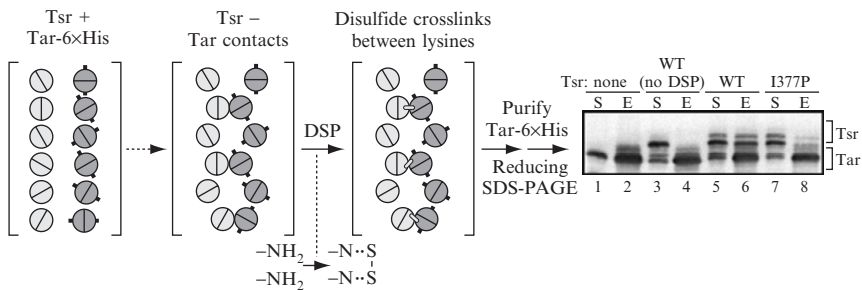


FIG. 2. Detection of interactions between receptor dimers with a lysine-reactive crosslinker. Cross-sections of receptor dimers are shown schematically as adjoining semicircles. Tsr (light) and Tar (dark) subunits do not form heterodimers, but do engage in dimer-dimer interactions detectable by DSP crosslinking. The Tar molecules carry a 6× His affinity tag (black rectangle) on each subunit that was used to purify Tar-containing crosslinking products before analyzing their composition by gel electrophoresis and immunoblotting. Samples labeled S were not affinity-purified; those labeled E were. Note that the DSP-mediated crosslinks were broken by reducing conditions before the gel analysis.

samples before (S) and after (E) elution from the nickel column, it is clear that the Tar-6× His molecules were efficiently retained by the nickel column (Fig. 2, lanes 2, 4, 6, and 8). The lower mobility Tsr band also appeared in the eluted samples, but only from DSP-treated cells (lane 6), not from untreated cells (lane 4). Thus, the presence of Tsr in the eluted material evidently depends on covalent connection(s) that DSP creates between His-tagged Tar and Tsr. Significantly, a mutant Tsr with a single amino acid replacement at a trimer contact residue (I377P) showed no DSP crosslinking to Tar-6× His (lane 8) even though the cellular level of the mutant protein was comparable to that of wild-type Tsr (compare lanes 5 and 7). These results suggested that DSP-mediated crosslinking between Tsr and Tar molecules could be based on a trimer-of-dimers interaction. This interaction was also detected in cells lacking all of the soluble chemotaxis proteins, including CheA and CheW, indicating that it was most likely a direct one between receptor molecules (Ames *et al.*, 2002).

A detailed description of the experiments (growth of cells, DSP treatment, cell disruption, membrane purification, solubilization of membrane proteins, purification of His-tagged proteins and crosslinked products on Ni-NTA matrix, gel electrophoresis, and Western blotting) can be found in Ames *et al.* (2002). Here, we emphasize three aspects of the experiments that are important to our conclusion that the observed crosslinking behavior reflects genuine interactions between different receptor dimers under normal physiological conditions. First, the 6× His tag at the C-terminus of Tar did not impair its chemotactic signaling ability, as judged by behavioral assays in soft agar plates, so Tar-6× His must be capable of the same protein-protein interactions as wild-type Tar. Second, Tar-6× His and wild-type Tsr were induced at levels optimal for wild-type function by each receptor. Thus, their interaction occurred under physiological conditions. Third, MCP molecules of different types do not seem to form heterodimers (Milligan and Koshland, 1988), implying that the observed crosslinking interactions occur between intact homodimers of both receptors.

Use of Cys-Targeted Crosslinking to Probe for the Trimer-of-Dimers Geometry in Cellular Chemoreceptor Assemblies

Tar and Tsr molecules have no native cysteine residues. We introduced cysteine reporters at positions that allowed us to exploit their unique sulfhydryl chemistry to look for trimer-of-dimer interactions in crosslinking experiments (Studdert and Parkinson, 2004). Inspection of the crystal structure of the Tsr cytoplasmic domain in which three different dimers closely interact at their hairpin tips (Kim *et al.*, 1999) (Fig. 1B) revealed

several general structural features that needed to be taken into account when devising crosslinking strategies to test whether a similar trimer-based interaction occurs between dimers *in vivo*.

First, the basic structural units in the trimer are homodimers, with two identical subunits. Residues in one subunit can mediate close contact between dimers at the trimer interface, whereas their counterparts in the other subunit will reside in a very different structural environment at the trimer perimeter. Thus, a residue in the inner subunit of a trimer may serve to stabilize the trimer, whereas the same residue in the outer subunit could play a different functional role, for example, promoting an interaction with CheA or CheW, which are known to bind to the tip of the receptor signaling domain (Fig. 1). However, due to the coiled-coil nature of the interaction between the two subunits of a dimer, cross-sections at different distances from the tip show that the positions of residues in the “inner” and “outer” subunits change relative to the trimer interface. For example, the methylation site residues in both subunits have roughly comparable orientations in the trimer.

Second, in the trimer-of-dimers crystal structure, the distances between specific residues and the solvent exposure of those residues can be precisely determined. Accordingly, cysteine reporter positions can be chosen on the basis of their predicted and differential propensity to form disulfides in dimers versus trimers of dimers.

In the following two sections, we describe how we used this approach to test the trimer-of-dimers organization of different receptors in chemotaxis-proficient cells. Importantly, every position chosen for a cysteine replacement was tested for its effects on receptor function in soft agar chemotaxis assays. Only reporter sites that had little or no deleterious functional effects were used for crosslinking studies. Except where otherwise indicated, experiments were performed in strains lacking CheA, CheW, CheR, and CheB proteins and the Cys-containing receptors were expressed at levels required for optimal function.

Intracytoplasmic Disulfide Crosslinks

Residues V384 and V398 lie at solvent-exposed positions far from their counterparts in the other subunit of the Tsr dimer (Fig. 3A and B). Moreover, in the trimer-of-dimers structure, neither residue lies close to its counterparts in the other dimers (Fig. 3A and B). However, V384 from the inner subunit of one dimer interacts closely with V398 from the outer subunit of a neighboring dimer (6.2 Å between alpha carbons) (Fig. 3C). The V384–V398 pair does not seem to represent a critical trimer contact, because it tolerates some amino acid replacements without loss of function

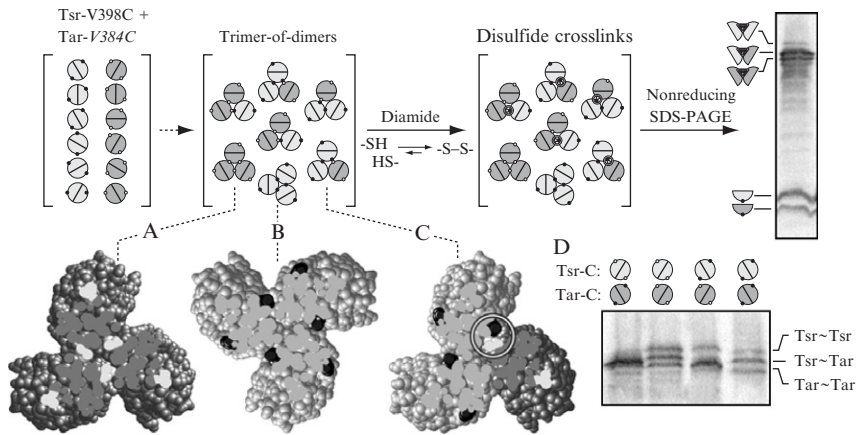


FIG. 3. Detection of trimer-based interactions between receptor dimers with cysteine-directed disulfide formation. Tsr and Tar dimers are depicted with the conventions described in Fig. 2. Their unique cysteine reporter sites are indicated by black (V398C) and white (V384C) circles. Cells expressing the two types of receptors at normal physiological levels were treated with diamide to render the cytoplasm more oxidizing and thereby promote disulfide bond formation. Crosslinked receptor subunits were analyzed by gel electrophoresis under nonreducing conditions and visualized by immunoblotting. (A) Expected arrangement of V384C reporter sites in a Tar trimer. (B) Expected arrangement of V398C reporter sites in a Tsr trimer. (C) Expected arrangement of V384C and V398C reporter sites in a mixed trimer containing both Tar and Tsr reporter molecules. Some of the reporter sites are much closer in the mixed trimer than in either of the pure trimers. (D) Crosslinked species generated by different combinations of Tsr and Tar reporter molecules. The mixed arrangements of reporter sites form disulfides much more efficiently than the others.

(Ames *et al.*, 2002). These structural and functional characteristics made V384 and V398 good candidates for probing higher-order chemoreceptor interactions *in vivo*. The trimer-of-dimers arrangement predicts that collisions between V384C and V398C reporters in different dimers should be much more frequent than V384–V384 or V398–V398 collisions. Some other higher-order receptor arrangements, for example, the “hedgerows” observed in a crystal structure of the signaling domain of an MCP molecule from *Thermotoga maritima* (Park *et al.*, 2006) make very different predictions about the proximity of the V384–V398 pair.

Based on these considerations, we created cysteine replacements at V384 and V398 in Tsr, and at the corresponding positions in Tar, and measured their ability to form interdimer disulfides by expressing different combinations of Cys-bearing receptors in the same cell, as summarized in Fig. 3 (Studdert and Parkinson, 2004). For simplicity, we refer to the Tar

reporters by the (italicized) numbers of the corresponding residues in Tsr. (The actual Tar residue numbers are two less than their Tsr counterparts.) Three of the reporters (Tsr-V398C, Tar-V384C, Tar-V398C) retained good signaling function; the fourth reporter (Tsr-V384C) had somewhat impaired function, but nevertheless exhibited crosslinking behavior comparable to that of its fully functional Tar counterpart. Here, we discuss the rationale behind these experiments and some technical aspects that need to be addressed in order to test the proximity of cytoplasmic reporter sites in proteins using disulfides as structural probes.

To obtain an unequivocal readout of interdimer crosslinking (as opposed to intradimer crosslinking between subunits of the same dimer), we monitored disulfide formation between the Tsr and Tar reporter molecules, which do not form heterodimers (see preceding text). In addition, we used a polyacrylamide gel system (10% acrylamide, 0.05% bis-acrylamide, pH 8.2) that augmented the different electrophoretic mobilities of Tar and Tsr (Feng *et al.*, 1997). Thus, we could distinguish crosslinked products containing two Tar subunits, or two Tsr subunits, or one subunit of each type. Tar \approx Tsr products should originate exclusively from interdimer collisions, whereas other crosslinked species could arise from either intra- or interdimer collisions.

As shown in the upper portion of Fig. 3, cells expressing Tar-V384C and Tsr-V398C formed three crosslinked receptor species, with the Tar \approx Tsr product more prominent than the Tar \approx Tar and Tsr \approx Tsr products. This result could reflect a trimer-of-dimers geometry for inter-receptor interactions, but alternatively could be due to preferential collisions between heterologous receptors, no matter what their higher-order arrangement. Tests with other reporter combinations excluded this alternate explanation (Fig. 3D). In the Tar-V384C + Tsr-V398C and Tar-V398C + Tsr-V384C combinations, the residues expected to interact in a trimer-of-dimers assembly are cysteines and should crosslink efficiently (Fig. 3C), whereas in the Tar-V398C + Tsr-V398C and Tar-V384C + Tsr-V384C combinations, both receptors have cysteines at equivalent positions. The trimer-of-dimers geometry predicts that these reporter sites should crosslink less efficiently (Fig. 3A,B). As Fig. 3D shows, when both members of the 384–398 pair were cysteines, the Tar \approx Tsr band predominated. When the same residue position in both Tar and Tsr carried the Cys reporter, the three possible crosslinking products formed with comparable efficiencies. This result is fully consistent with the trimer-of-dimers geometry of chemoreceptor assemblies, but cannot exclude other possible arrangements. However, any proposed alternative arrangement must be able to account for the preferential crosslinking of V398 and V384 residues. This is not the case for the hedgerow arrangement of the cytoplasmic domain of a *T. maritima* MCP (Park *et al.*, 2006), for example. In that structure, the distances

between the 384 and 398 positions were not significantly less than the 398–398 or the 384–384 distances. Conceivably, the MCP arrangements could differ between *E. coli* and *T. maritima*, but it seems equally likely that the apparent disagreement reflects differences in crystal packing interactions rather than real physiological differences. Only *in vivo* crosslinking studies conducted in *Thermotoga*, as well as in other species, can resolve these issues.

Technical Considerations

The position of the bridging disulfide bond between receptor subunits can create small but consistent differences in mobility between various crosslinking products (Fig. 3D). Crosslinked products migrate faster with a disulfide near the subunit termini than with a connection near their centers, which creates a more “H”-shaped molecule (compare Tar-V398C \approx Tsr-V398C with Tar-V384C \approx Tsr-V384C in Fig. 3D).

The highly reducing nature of the cytoplasm opposes disulfide bond formation *in vivo* (Ritz and Beckwith, 2001). To perform the experiments just described, we had to create a less reducing cellular environment. To this end, cells were harvested at late-log phase of growth, resuspended in KEP buffer [10 mM potassium phosphate (pH 7), 0.1 mM EDTA] at an $OD_{600} = 2$, and incubated at 30° for 45 min in the presence of 0.5 mM diamide. Treatment with this thiol-specific oxidant (Kosower and Kosower, 1995) greatly enhanced the detection of intracytoplasmic disulfide bonds. Before lysis of the cells, the unreacted sulfhydryl groups were quenched by treatment with 10 mM NEM. Lysis buffer also contained NEM to avoid the formation of disulfides during processing of samples.

A Trifunctional Cys-Targeted Crosslinker

Above the trimer contact region, the three dimers of the trimer splay apart, forming a solvent-accessible space along the central axis of the trimer (Fig. 4A). We reasoned that, if the crystal structure represents the interactions that occur *in vivo*, it might be possible to capture all three axial subunits of a trimer with TMEA, a tri-functional thiol-specific crosslinking agent (Fig. 4C), provided that the target cysteines are appropriately positioned. The thiol-reactive maleimide groups in TMEA lie 10.3 Å apart, so we tested comparably spaced residues in the Tsr trimer as reporter sites. A cysteine replacement at S366 proved best. The alpha-carbons at this position lie 12.3 Å from each other in the subunits facing the central space, whereas those on the outside of the trimer are very far apart and shielded from one another by the bulk of the trimer (Fig. 4B).

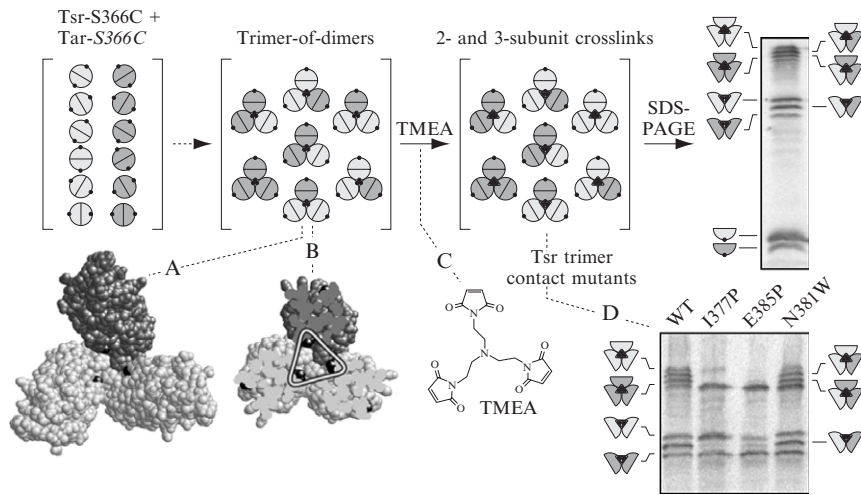


FIG. 4. Detection of trimer-based interactions between receptor dimers with a trifunctional cysteine-targeted crosslinker. Tsr and Tar dimers are depicted with the conventions described in Fig. 2 and Fig. 3. Cells expressing normal physiological levels of Tar and Tsr molecules with a cysteine reporter (S366C) were treated with TMEA (structure shown in [C]). TMEA-crosslinked receptor subunits were analyzed by gel electrophoresis and visualized by immunoblotting. (A) Arrangement of reporter sites in a mixed trimer, viewed from the cell membrane toward the cytoplasmic tip of the trimer. Reporter sites (black atoms) lie close together at the trimer axis, but far apart (not visible) in the outside subunits of the dimers. (B) Cross-section view of a mixed trimer showing the close-spaced triangular arrangement of reporter sites in the inside subunits of the dimers. (D) TMEA crosslinking patterns of wild-type (WT) and mutant Tsr reporter molecules when mixed with a wild-type Tar reporter. The mutant molecules carry single amino acid replacements at one of the trimer contact residues. The I377P and E385P lesions disrupt trimer formation; the N381W lesion does not.

Most importantly, Tsr and other receptors with a cysteine replacement at this position retained full signaling function.

Receptors with the S366C reporter generated two- and three-subunit crosslinking products upon treatment of whole cells with TMEA (Studdert and Parkinson, 2004). Cells were simply harvested, resuspended in KEP buffer, treated for 5 to 20 s with 50 μ M TMEA, and lysed after quenching the reaction with 10 mM NEM. Then, the products were analyzed by SDS-PAGE and Western blotting with an anti-MCP antibody. A typical TMEA experiment with cells expressing both Tsr-S366C and Tar-S366C is shown in the upper portion of Fig. 4. Assuming that the 2- and 3-subunit crosslinking products represent TMEA-trapped inner subunits from trimers of different compositions (see supporting considerations in the following text), the

distribution of crosslinked products was consistent with random formation of trimers from the available dimer pool. Thus, trimer composition would only depend on the relative abundance of the different receptor dimers (for theoretical predicted composition of trimers, see Fig. 5C). This assumption was experimentally tested by expressing Cys-containing Tar and Tsr receptors at different relative levels of expression and analyzing the distribution of crosslinked products upon TMEA treatment (Studdert and Parkinson, 2004). The results were clearly consistent with random mixing of dimers, with receptors expressed at a low level being found almost exclusively in mixed crosslinked species. Random assembly of trimers from the pool of receptor dimers implies that receptor types in relatively low cellular abundance should reside mainly in mixed trimers with higher abundance receptor types. The TMEA crosslinking behavior of the low abundance Trg (Studdert and Parkinson, 2004) and Aer (Gosink *et al.*, 2006) receptors supported this view.

Technical Considerations About TMEA Treatment of Cells

TMEA treatments as short as 5 s and as long as 2 h produced similar extents and patterns of crosslinking. Higher TMEA concentrations had no enhancing effect on the yield of crosslinking products. Thus, TMEA seems to react rapidly with all receptor subunits that are available for crosslinking, yielding a “snapshot” of the higher-order structure of the receptor population.

Intact and broken cells exhibit very different TMEA behaviors. Cells expressing receptors at physiological levels yielded crosslinking products with high and reproducible efficiency, whereas membrane preparations from the same cells did not yield any crosslinking product (Studdert and Parkinson, 2004). TMEA treatment of membrane preparations was only effective if the receptors had been highly overexpressed. We hypothesize that cell disruption destabilizes interactions between receptors that can be restored or mimicked by dense crowding. Those interactions may be important for signaling because receptor crowding is also needed to activate CheA *in vitro*.

Evidence That TMEA Traps the Axial Subunits of Trimers

Formation of TMEA crosslinking products was not dependent on the presence of CheA and CheW (Studdert and Parkinson, 2004). In the absence of those proteins, receptor clusters are less tight (Kentner *et al.*, 2006; Lybarger and Maddock, 2000), whereas direct interactions between receptors seem to be unaffected (Ames *et al.*, 2002).

Tsr-S366C derivatives carrying loss-of-function lesions at trimer contact residues (e.g., I377P, E385P) were defective in forming 3-subunit TMEA products when expressed alone (Studdert and Parkinson, 2004) or mixed

TMEA products when coexpressed with Tar-S366C (Fig. 4D). In contrast, mutant Tsr molecules with epistatic trimer contact lesions (e.g., N381W), which impair the function of wild-type Tar and other receptors, still formed TMEA crosslinking products, both alone (Studdert and Parkinson, 2004) and when coexpressed with Tar-S366C (Fig. 4D). The crosslinking phenotypes of mutant Tsr receptors are fully consistent with their functional properties. Loss-of-function mutants evidently cannot form trimers, whereas epistatic mutants probably form defective trimers that impair the function of other receptors in the cluster (Ames *et al.*, 2002).

TMEA Competition Assay: A Tool for Assessing the Trimer-Forming Ability of Mutant Receptors

The trimer-based interpretation of our TMEA crosslinking results predicts that high relative levels of a receptor with no cysteine reporter (a competitor) should decrease the crosslinking products from a receptor with a TMEA reporter site. To simplify these competition experiments, we built a strain with a chromosomally encoded Tar-S366C (Tar•C) reporter and no other receptors (Studdert and Parkinson, 2005). In this host, we expressed different levels of wild-type or mutant Tsr molecules and examined the TMEA crosslinking pattern of Tar•C (Fig. 5A). We expected that Tsr molecules able to join mixed trimers of dimers would cause a corresponding decrease in interdimer-dependent TMEA products (Fig. 5A, trimer-proficient Tsr), whereas Tsr mutants with defects in interreceptor interactions would not interfere with the formation of any Tar•C crosslinking products (Fig. 5A, trimer-deficient Tsr). We found clear examples of both categories of mutants: For example, high levels of Tsr-N376W completely suppressed Tar•C crosslinking products, whereas comparable levels of Tsr-I377P had no effect on Tar•C crosslinking (Fig. 5A).

Several conclusions can be drawn from these competition experiments:

The competition results support our interpretation of direct TMEA crosslinking results. Conceivably, a mutant receptor could appear to be trimer-defective in direct TMEA tests if the mutation simply altered the orientation of the reporter site. However, this explanation can be excluded if the same mutant receptor fails to compete with Tar•C for mixed trimer formation, as proved to be the case for the prototypical trimer-defective lesion, I377P.

TMEA products mainly arise from *interdimer* crosslinking events. Formation of crosslinks between the subunits of a dimer should not be subject to competition by a heterologous receptor because Tar and Tsr do not form heterodimers. Yet, trimer-proficient competitors blocked all Tar•C crosslinking products. Thus, both the 2- and 3-subunit TMEA products of

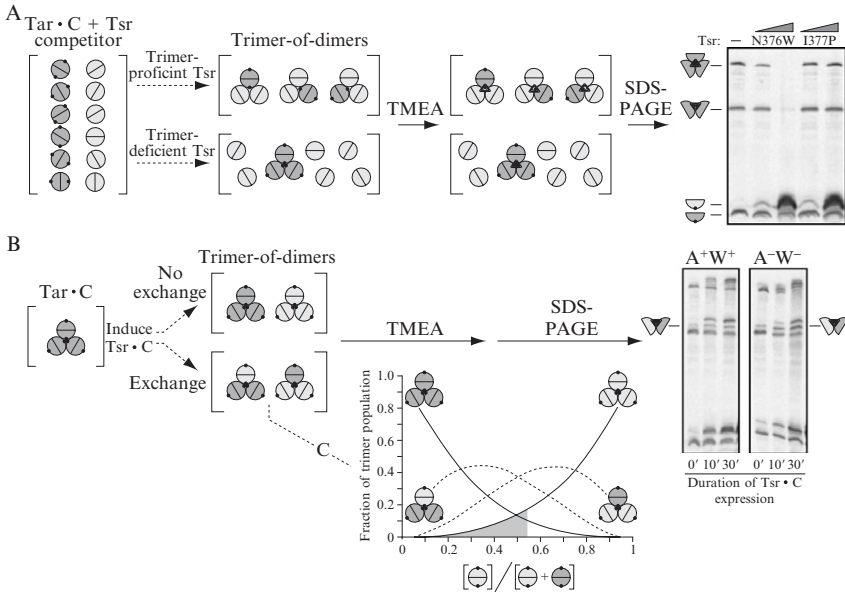


FIG. 5. Assessing receptor-receptor interactions with crosslinking competition and exchange assays. Tsr and Tar dimers are depicted with the conventions described in Figs. 2, 3, and 4. (A) Competition assay for evaluating the trimer-forming ability of Tsr molecules that do not bear a cysteine reporter site. Cells expressing a physiological level of Tar molecules with the S366C reporter (Tar·C) and different levels of a Tsr competitor were treated with TMEA and analyzed as described in Fig. 4. High levels of trimer-proficient Tsr molecules (e.g., N376W) prevent Tar crosslinking, whereas trimer-deficient Tsr mutants (e.g., I377P) do not. (B) Exchange assay for evaluating the stability of preformed trimers. Cells were allowed to express a Tar·C reporter at physiological levels for many generations, then induced for expression of a Tsr·C molecule, treated with TMEA, and the receptor crosslinking products analyzed by gel electrophoresis and immunoblotting. (C) Expected proportions of different trimer compositions if preexisting trimers freely exchange members with the pool of newly synthesized receptor molecules. The exchange assay is most sensitive at relatively low levels of newly made receptors (shaded portion of plot). Exchange efficiency was quantified by comparing the observed and expected proportions of mixed and pure two-subunit crosslinking products. Note that trimer exchanges occur much more readily in cells lacking the CheA and CheW proteins.

trimer-proficient receptors arise from *interdimer* crosslinks. Some mutant receptors (e.g., Tsr-I377P) cannot form trimer-based crosslinks, but do form *intradimer* crosslinks, due presumably to destabilization of the receptor tip where the mutation lies.

Because a competing receptor does not require a TMEA reporter site, the competition assay offers a simple method for assessing the trimer-forming

potential of any mutant receptor. It could even be used to test heterologous receptors from other organisms, for example, *T. maritima* MCPs, for trimer-based interactions with the Tar•C reporter.

The competition assay should also serve to identify receptors with different types of trimer-forming defects. For example, some trimer-defective mutant receptors may be tolerated as a single member of a mixed trimer. Mutant receptors of this sort would be expected to cause a drastic decrease in the 3-subunit Tar•C crosslinking product and a concomitant increase in the 2-subunit crosslinking product.

Exchange Assay: Dynamic Changes in Trimer Composition as a Consequence of Changes in the Receptor Population

The TMEA crosslinking assay provides a snapshot of trimer groupings in the cell, which, in turn, reflects the composition of the entire receptor population. To explore the cellular stability of receptor trimers of dimers, we devised an exchange assay (Fig. 5B) for following the fate of established trimers upon a change in composition of the receptor population (Studdert and Parkinson, 2005). In this assay, a strain carrying a constitutively expressed, chromosomally encoded Tar•C reporter and an IPTG-inducible Tsr•C plasmid was grown to midlog phase and then induced for Tsr•C expression. The cells were treated with TMEA at different times after the onset of induction and their crosslinking products examined. If the preformed Tar•C trimers are highly dynamic, then the composition of trimers after Tsr•C induction should depend entirely on the relative cellular levels of the two receptor types, as depicted in Fig. 5B (exchange alternative). In this case, many of the newly made Tsr•C molecules should be found in mixed trimers, which would yield mixed crosslinking products. However, if preformed Tar•C trimers are stable, more of the newly made Tsr•C molecules should be found in pure crosslinking products (Fig. 5B, no exchange alternative). Thus, to assess the exchangeability of newly made Tsr•C dimers with the preexisting Tar•C population, we compared the measured levels of mixed crosslinking products with those predicted by purely random mixing (Fig. 5C). TMEA treatment was performed at short induction times, when the levels of Tsr•C were relatively low, to maximize the expected difference between the two exchange patterns (Fig. 5C, shaded region).

Although previous experiments showed that CheA and CheW were not required for trimer formation, exchange assays showed that these proteins made trimers exchange-resistant (Fig. 5B). In cells containing both CheA and CheW, pure 2- and 3-subunit crosslinking products were relatively more abundant than mixed crosslinking products. In cells lacking both proteins (or either one, not shown), mixed crosslinking products were

relatively more abundant. These differences were most evident in the two-subunit products, for which we defined an “exchange factor” as the ratio of the observed to predicted levels of the $\text{Tar}\cdot\text{C} \approx \text{Tsr}\cdot\text{C}$ product. For the experiment shown in Fig. 5B, the exchange factor for cells lacking CheA and CheW was 0.95, indicative of nearly free exchange between new and old receptor molecules. In contrast, the exchange factor for cells that contained CheA and CheW was 0.35, indicating that the newly made Tsr·C receptors were not freely exchanging with the preexisting Tar·C population. The low-exchange crosslinking pattern persisted for up to 3 h when protein synthesis was inhibited before the TMEA treatment. Moreover, the presence of attractants (serine, aspartate, or both) in the incubation buffer did not increase receptor exchangeability. We conclude that receptors synthesized in the presence of both CheA and CheW assemble into an exchange-resistant complex based on trimers of dimers and that attractant stimuli do not alter the low exchangeability of preassembled receptor trimers.

Concluding Remarks

The experimental approaches described in this chapter were aimed at characterizing the higher-order organization of chemoreceptors in unperturbed cells. To that end, we reproduced normal *in vivo* stoichiometries as much as possible to minimize physiologically irrelevant collisional interactions between receptors. Our experimental designs were guided by the crystal structure of the cytoplasmic domain of Tsr and explored the premise that receptors form trimer-of-dimer arrangements in living cells. These *in vivo* crosslinking experiments have served to

- demonstrate direct interactions between both homologous and heterologous receptors that are not dependent on other chemotaxis signaling proteins (DSP, disulfides, TMEA).
- reveal crosslinking patterns consistent with the proposed trimer-of-dimers geometry for receptor–receptor interactions (disulfides, TMEA).
- demonstrate that amino acid replacements at trimer interface residues disrupt higher-order receptor interactions (DSP, disulfides, TMEA: direct and competition-based).
- define the conditions that promote or inhibit the exchangeability of dimers between trimers.

Disulfide crosslinking of cysteine reporters in the periplasmic domain of Tar has also been used to investigate higher-order receptor interactions in intact cells (Homma *et al.*, 2004; Irieda *et al.*, 2006). Those studies are consistent with a close interaction among three receptor dimers, but unlike

the cytoplasmic contacts in trimers of dimers, the efficiency of periplasmic crosslinking was highly dependent on the presence of CheA and CheW and the crosslinking efficiency changed upon addition of attractant. It seems likely that these periplasmic interactions occur between members of different trimers of dimers, for example, through a receptor arrangement in which the periplasmic domains of each member of a trimer abut the periplasmic domains of dimers from other trimers in the receptor array (Kim *et al.*, 2002). In such an array arrangement, the periplasmic interactions between receptors, unlike the relatively static association of signaling domains in the cytoplasmic tip of a trimer, might depend on intertrimer bridging connections provided by CheA and CheW, which could be affected by the signaling state of the receptors. Indeed, using other periplasmic reporter sites, Irieda *et al.* (2006) observed changes in crosslinking efficiency that were consistent with stimulus-induced rotational movements of the individual receptor dimers in the array.

It should be possible to reconcile the structural information provided by periplasmic and cytoplasmic crosslinking approaches with additional *in vivo* studies that utilize both types of reporter sites. Other promising areas for investigation include crosslinking tests of the recently determined structure for a HAMP domain (Hulko *et al.*, 2006) and a search for cytoplasmic reporter sites that are sensitive to the receptor's signaling or modification state.

In vivo crosslinking approaches are one of the few experimental options available for exploring the structure of receptor signaling complexes in their native context. When combined with genetic and physiological studies, the crosslinking techniques described in this chapter should lead to a detailed molecular understanding of structure–function relationships in chemoreceptors. Similar approaches should be applicable to other protein–protein interactions.

Acknowledgments

Research in the authors' laboratories is funded by grant GM19559 from the National Institute of General Medical Sciences and by TW07216, a Fogarty International Research Collaboration Award.

References

- Ames, P., Studdert, C. A., Reiser, R. H., and Parkinson, J. S. (2002). Collaborative signaling by mixed chemoreceptor teams in *Escherichia coli*. *Proc. Natl. Acad. Sci. USA* **99**, 7060–7065.
- Bray, D., Levin, M., and Morton-Firth, C. (1998). Receptor clustering as a cellular mechanism to control sensitivity. *Nature* **393**, 85–88.
- Chelsky, D., and Dahlquist, F. W. (1980). Chemotaxis in *Escherichia coli*: Associations of protein components. *Biochemistry* **19**, 4633–4639.

- Feng, X., Baumgartner, J. W., and Hazelbauer, G. L. (1997). High- and low-abundance chemoreceptors in *Escherichia coli*: Differential activities associated with closely related cytoplasmic domains. *J. Bacteriol.* **179**, 6714–6720.
- Gestwicki, J. E., Lamanna, A. C., Harshey, R. M., McCarter, L. L., Kiessling, L. L., and Adler, J. (2000). Evolutionary conservation of methyl-accepting chemotaxis protein location in Bacteria and Archaea. *J. Bacteriol.* **182**, 6499–6502.
- Gosink, K. K., Buron-Barral, M., and Parkinson, J. S. (2006). Signaling interactions between the aerotaxis transducer Aer and heterologous chemoreceptors in *Escherichia coli*. *J. Bacteriol.* **188**, 3487–3493.
- Homma, M., Shiomi, D., and Kawagishi, I. (2004). Attractant binding alters arrangement of chemoreceptor dimers within its cluster at a cell pole. *Proc. Natl. Acad. Sci. USA* **101**, 3462–3467.
- Hulko, M., Berndt, F., Gruber, M., Linder, J. U., Truffault, V., Schultz, A., Martin, J., Schultz, J. E., Lupas, A. N., and Coles, M. (2006). The HAMP domain structure implies helix rotation in transmembrane signaling. *Cell* **126**, 929–940.
- Irieda, H., Homma, M., and Kawagishi, I. (2006). Control of chemotactic signal gain via modulation of a pre-formed receptor array. *J. Biol. Chem.* **281**, 23880–23886.
- Kentner, D., Thiem, S., Hildenbeutel, M., and Sourjik, V. (2006). Determinants of chemoreceptor cluster formation in *Escherichia coli*. *Mol. Microbiol.* **61**, 407–417.
- Kim, K. K., Yokota, H., and Kim, S. H. (1999). Four-helical-bundle structure of the cytoplasmic domain of a serine chemotaxis receptor. *Nature* **400**, 787–792.
- Kim, S. H., Wang, W., and Kim, K. K. (2002). Dynamic and clustering model of bacterial chemotaxis receptors: Structural basis for signaling and high sensitivity. *Proc. Natl. Acad. Sci. USA* **99**, 11611–11615.
- Kosower, N. S., and Kosower, E. M. (1995). Diamide: An oxidant probe for thiols. *Methods Enzymol.* **251**, 123–133.
- Lybarger, S. R., and Maddock, J. R. (2000). Differences in the polar clustering of the high- and low-abundance chemoreceptors of *Escherichia coli*. *Proc. Natl. Acad. Sci. USA* **97**, 8057–8062.
- Maddock, J. R., and Shapiro, L. (1993). Polar location of the chemoreceptor complex in the *Escherichia coli* cell. *Science* **259**, 1717–1723.
- Milburn, M. V., Prive, G. G., Milligan, D. L., Scott, W. G., Yeh, J., Jancarik, J., Koshland, D. E., Jr., and Kim, S. H. (1991). Three-dimensional structures of the ligand-binding domain of the bacterial aspartate receptor with and without a ligand. *Science* **254**, 1342–1347.
- Milligan, D. L., and Koshland, D. E., Jr. (1988). Site-directed cross-linking. Establishing the dimeric structure of the aspartate receptor of bacterial chemotaxis. *J. Biol. Chem.* **263**, 6268–6275.
- Park, S. Y., Borbat, P. P., Gonzalez-Bonet, G., Bhatnagar, J., Pollard, A. M., Freed, J. H., Bilwes, A. M., and Crane, B. R. (2006). Reconstruction of the chemotaxis receptor-kinase assembly. *Nat. Struct. Mol. Biol.* **13**, 400–407.
- Parkinson, J. S., Ames, P., and Studdert, C. A. (2005). Collaborative signaling by bacterial chemoreceptors. *Curr. Opin. Microbiol.* **8**, 116–121.
- Ritz, D., and Beckwith, J. (2001). Roles of thiol-redox pathways in bacteria. *Annu. Rev. Microbiol.* **55**, 21–48.
- Sourjik, V. (2004). Receptor clustering and signal processing in *E. coli* chemotaxis. *Trends Microbiol.* **12**, 569–576.
- Sourjik, V., and Berg, H. C. (2000). Localization of components of the chemotaxis machinery of *Escherichia coli* using fluorescent protein fusions. *Mol. Microbiol.* **37**, 740–751.

- Sourjik, V., and Berg, H. C. (2002). Receptor sensitivity in bacterial chemotaxis. *Proc. Natl. Acad. Sci. USA* **99**, 123–127.
- Sourjik, V., and Berg, H. C. (2004). Functional interactions between receptors in bacterial chemotaxis. *Nature* **428**, 437–441.
- Studdert, C. A., and Parkinson, J. S. (2004). Crosslinking snapshots of bacterial chemoreceptor squads. *Proc. Natl. Acad. Sci. USA* **101**, 2117–2122.
- Studdert, C. A., and Parkinson, J. S. (2005). Insights into the organization and dynamics of bacterial chemoreceptor clusters through *in vivo* crosslinking studies. *Proc. Natl. Acad. Sci. USA* **102**, 15623–15628.
- Szurmant, H., and Ordal, G. W. (2004). Diversity in chemotaxis mechanisms among the bacteria and archaea. *Microbiol. Mol. Biol. Rev.* **68**, 301–319.
- Zhulin, I. B. (2001). The superfamily of chemotaxis transducers: From physiology to genomics and back. *Adv. Microb. Physiol.* **45**, 157–198.